Dicke superradiance and stimulated electronic Raman scattering of indium

Santaram Chilukuri

Purdue University North Central, Westville, Indiana 46391

Dicke superradiance (SR) and stimulated electronic Raman scattering (SERS) have been observed at 451.1 nm in atomic indium following optical excitation at the resonance line 410.2 nm. The SR and SERS characteristics have been studied. The coherent population trapping state was observed. The pump to Raman conversion efficiency is found to be up to 40% and a range of tunability of 30 cm^{-1}. The SR and SERS processes have shown different optimum densities of indium atoms. [S1050-2947(96)04407-1]

Superradiance (SR) is the cooperative emission from a large number of two-level atoms initially in an inverted state, with peak radiation power proportional to the square of the number of emitting atoms. Cooperative radiation was qualitatively predicted by Dicke [1] and has been observed in several laboratories [2] since 1972.

We report here our experimental results of the observed superradiance and stimulated electronic Raman scattering (SERS) of indium vapor. The experimental arrangement is shown in Fig. 1. Quartz cells of lengths 5 to 60 cm with flat windows were sealed with a small amount of indium metal held in an appendage. The tube was placed in a specially designed oven. There was provision in the oven to make observations perpendicular to the tube axis. Two heat plugs kept the windows clean. An yttrium aluminum garnet (YAG) pumped Molectron dye laser aligned along the axis of the tube provided the excitation. The pump pulse energy was 25 μJ, the linewidth 0.1 Å, the duration 3 ns, and the repetition rate 20 Hz. A Corning plate (5128F) filtered the pump pulse at 410 nm but allowed the radiation at 451 nm.

The low-lying levels of indium atoms are shown in Fig. 2. The laser was tuned to the resonance line of indium at 410.2 nm, selectively exciting atoms to the $6\,^2S$ state and producing inverted population between the $6\,^2S$ state and the $5\,^2P_{3/2}$ state. At low excited atom density N the atomic dipoles remain independent of each other and the sample radiates an isotropic fluorescence signal proportional to N with delay time T_1, the inverse of the Einstein A coefficient of the usual spontaneous emission. This is ordinary fluorescence and the radiation is incoherent. We detected the fluorescence signal at 451.1 nm at indium densities of 8.6×10^8 atoms/cm^3 or higher. The fluorescence signal was monitored perpendicular to the tube axis using a monochromator set to 451 nm. However, at large enough N, the dipoles of the different atoms start interacting with each other through their common coupling with the axial modes of the radiation field, the characteristic coupling time being $T_r = 8\pi A T_1(\lambda^2 N)^{-1}$ expressed in terms of the cross-sectional area A of the excited region and the transition wavelength λ and having a value $\cong 0.05$ ns. After a delay time T_D proportional to T_r, all the dipoles strongly lock in phase with each other and radiate along the axis of the active medium, a light pulse with an intensity proportional to N^2. The phenomenon is observable only if T_r is shorter than the dephasing time T_2 of the atomic dipoles. The dominating dephasing process is the Doppler effect and $T_2 \cong 1$ ns. The delay time T_D of the superradiant emission exceeds T_r and T_2. In our experiments, coherent superradiant pulses of 1.5 to 2 ns in the forward direction were observed at or above an indium density of 3×10^{11} atoms/cm^3. The SR pulse intensity measured as a function of the square of indium density is shown in Fig. 3. The data represent average values measured at the half maximum point of the pulses. It shows a threshold of about 3×10^{11} atoms/cm^3 for the onset of SR. In the density range of 3×10^{11} to 1.5×10^{12} atoms/cm^3, the SR intensity shows a clear N^2 dependence, as expected for Dicke superradiance. The fluorescence signal at 451 nm monitored perpendicular to the tube axis versus the number density of indium atoms is shown in Fig. 4. The dots represent the experimental data points in all plots and the smooth, solid lines drawn to guide the reader's eye. The fluorescence signal was detected at
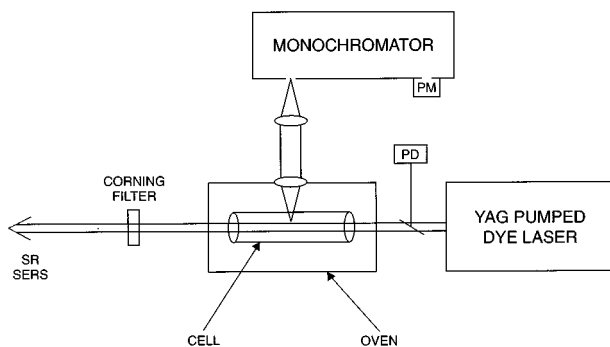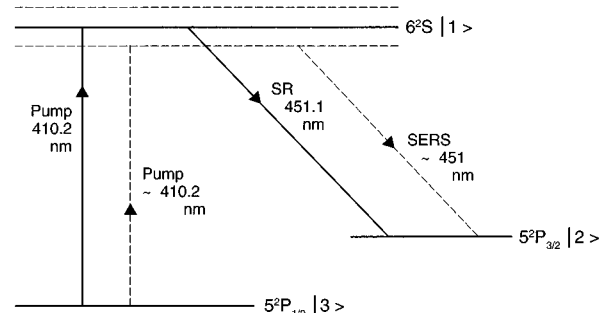

FIG. 1. Experimental arrangement.

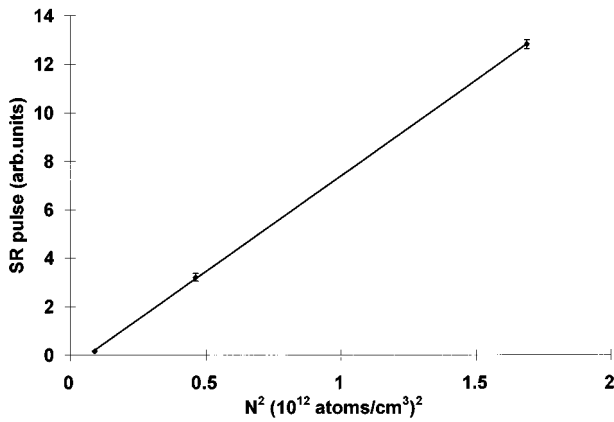FIG. 2. Level scheme of indium for SR and SERS.

FIG. 3. SR pulse intensity as a function of the square of the number density of indium atoms. The indium cell length is 25 cm.

indium densities of 8.6×10^8 atoms/cm^3 or higher. There is a clear leveling off of the fluorescence intensity at the onset of superradiance. When the sample is superradiant, the atoms are coupled to emit along the axis of the active medium and as a result the normal isotropic fluorescence will level off. The polarizations of the SR pulse both parallel and perpendicular to the pump pulse were separately measured. The parallel component is predominant, about 12 times stronger than the perpendicular component. Two photodiodes, spatially separated, one monitoring the pump pulse and other the SR pulse, were used with an oscilloscope to measure the time delay. The spatial separation of the photodiodes contributed a 3-ns delay. The time delay between the SR pulse and the pump pulse measured as a function of pump pulse intensity is shown in Fig. 5. Neutral density filters were used to vary the pump pulse intensity. The time delay decreased with increasing pump intensity. At higher intensities of the pump, N (the excited atom density) would increase and the characteristic coupling time T_r and consequently T_D would decrease. The delay time was also found to scale inversely with the number density of excited indium atoms. These results are in agreement with the theoretical predictions of superradiance.

Stimulated electronic Raman scattering (SERS) was first

FIG. 5. Time delay between the pump pulse and the SR pulse plotted versus $1/I$ where I is the intensity of the pump pulse. The delays shown include the 3-ns contribution from the spatial separation of the photodiodes. The indium cell length is 25 cm.

observed in potassium vapor by Rokni and Yatsiv [3]. It has been demonstrated in several other studies [4] that useful Raman radiation is enhanced by the resonant intermediate levels. SERS in indium vapor was first reported by Takubo *et al.* [5], who investigated behaviors of $5P_{1/2}$-$5P_{3/2}$ SERS. We report the results of our study of stimulated electronic Raman scattering of indium vapor, which generally confirm the earlier observations of Tabuko *et al.* We observed SERS of indium $5P_{1/2}$-$5P_{3/2}$ in the forward direction around an indium density of 10^{13} atoms/cm^3 or higher. The levels involved are shown in Fig. 2. The oscillator strengths f_{ik} of the transitions $5\,^2P_{1/2}-6\,^2S$ and $5\,^2P_{3/2}-6\,^2S$ are 0.137 and 0.157, respectively, and the relative line strength $S_{3/2}/S_{1/2}$ is 2.42 [6]. The power gain of the SERS radiation for a length l of vapor cell is $\exp(gIl)$ where the gain coefficient g is given by [4,7]
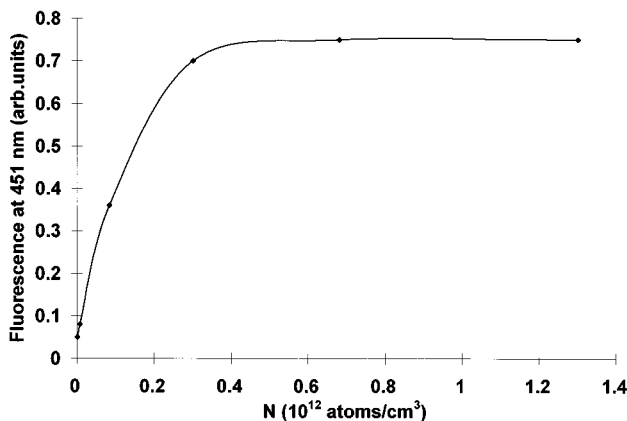

FIG. 4. Fluorescence monitored perpendicular to the 25-cm-long cell as a function of indium number density. The fluorescence intensity levels off with the onset of SR.
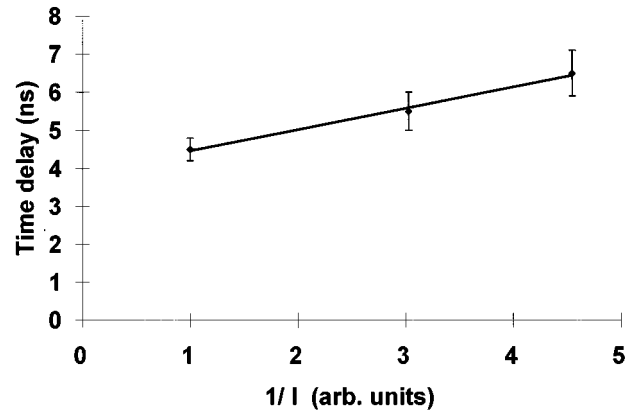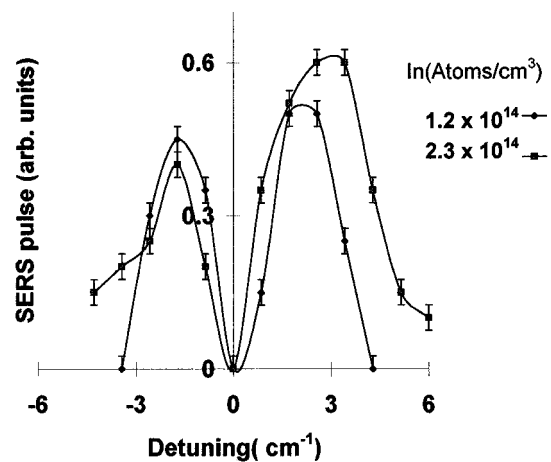

FIG. 6. SERS pulse as a function of detuning from the line center for two different indium densities. The output is large on either of side of the atomic line center. The dip at the line center is due to coherent population trapping. The range of tunability increased with increasing density of indium atoms. The indium cell length is 45 cm. The output measured with a Power meter.
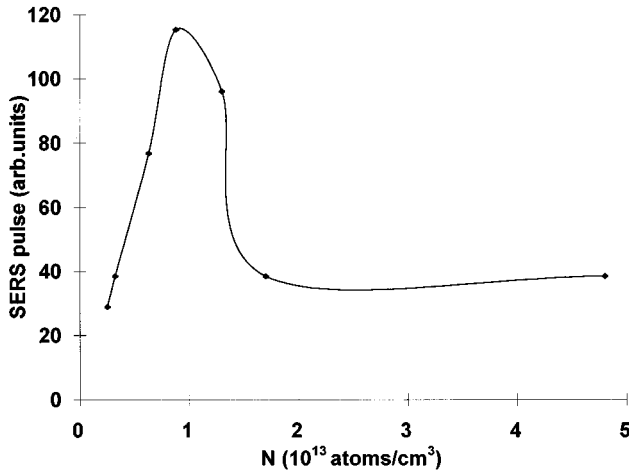
FIG. 7. SERS pulse versus number density of indium. Note that the pump pulse is tuned to the line center and the output measured with a photodiode. In the density range of 2×10^{12} to 9×10^{12} both SR and SERS are competing. SERS is totally responsible for the output around 10^{13} atoms/cm^3. The subsequent decrease in intensity is due to the evolution of a CPT state. The cell length is 25 cm.

$$g = \frac{Ne^4 \nu_s f_{12} f_{13}}{32\pi^2 \varepsilon_0^2 hc^2 m_e^2 \nu_{12} \nu_{13} (\nu_{13} - \nu_p)^2 \Gamma}, \quad (1)$$

where all quantities are in standard metric units (meter, kilogram, second, ampere), N is the density of indium atoms, I the intensity of the pump (W/m^2), and all frequencies including the stokes linewidth Γ are expressed in Hertz. A Fabry-Pérot interferometer was used to examine the SERS output. It clearly showed expanding or collapsing fringes as the pump wavelength is tuned, demonstrating the tunability of SERS output. The SERS output pulse energy as a function of detuning for two different indium densities is shown in Fig. 6. The output is large on either side of the atomic line center. There is a dip in the SERS output at the line center. Indeed, a similar dip at the line center was observed in several other atomic systems. A power meter was used to measure the output for Fig. 6. The power meter was not sensitive at low powers, it read zero below a certain threshold. Though small, there always was a SERS output when the laser was tuned to the line center, seen both visually and observed using a photodiode. We show that coherent population trapping (CPT) is responsible for the dip [8]. Quantum coherence and interference in atomic systems have been shown to lead to interesting optical phenomena. Among the many recent discoveries are electromagnetically induced transpar-
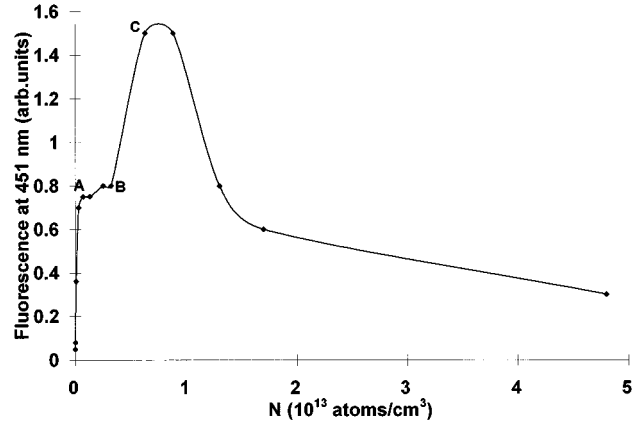

FIG. 8. Fluorescence monitored perpendicular to the tube axis at 451 nm versus indium number density. Note that the pump pulse is tuned to the line center. Density range A to B is the SR regime. C and beyond is the SERS regime. Fluorescence intensity drops in the SERS regime due to CPT. The cell length is 25 cm.

ency, lasing without population inversion, and the potential generation of a large absorptionless index of refraction. A three-level Λ system with two closely spaced ground levels optically coupled to a common excited level by two coherent fields gives rise to trapping of population in a coherent superposition of the ground levels, which is immune to further excitation. The nonabsorbing coherent superposition state is called the CPT state and this occurs whenever the frequency separation between the two fields is equal to the separation between the ground levels. It is especially strong when the detuning is zero and the two external fields are exactly on resonance with the respective atomic transitions. The evolution of the CPT state is dependent on the relative strength of the fields and the spontaneous decays involved. For strong fields and for the spontaneous decay rate from state $|1\rangle \leftrightarrow |2\rangle$, greater than for state $|1\rangle \leftrightarrow |3\rangle$ the time taken to reach the steady state (CPT) is relatively less [9]. Here the two driving fields are the pump laser field and the Stokes field. Our experiments confirm the evolution of the CPT state. Figure 7 shows the SERS (and SR) output of indium measured with a photodiode when the pump pulse is tuned to the line center using a 25-cm-long indium cell. It shows an increase in intensity in the density range of 2×10^{12} to 9×10^{12} atoms/cm^3. However, in this density regime, the output is no longer linear with N^2 and barely begins to show a tuning range for the pump pulse. Both SR and SERS processes coexisted in this range with the SERS process totally
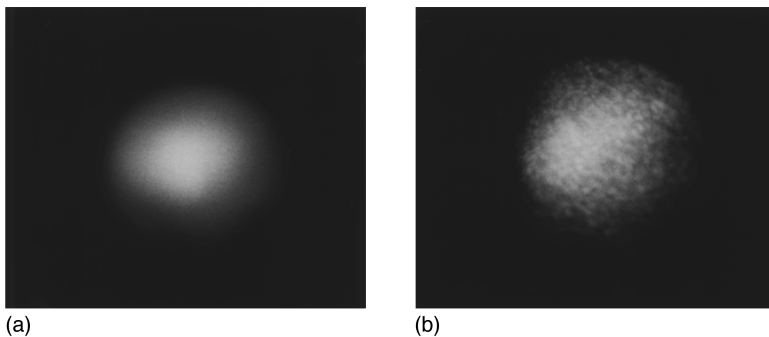

(a)

(b)

FIG. 9. Photograph of the SERS output viewed on a screen at the peak corresponding to (a) positive detuning and (b) negative detuning.
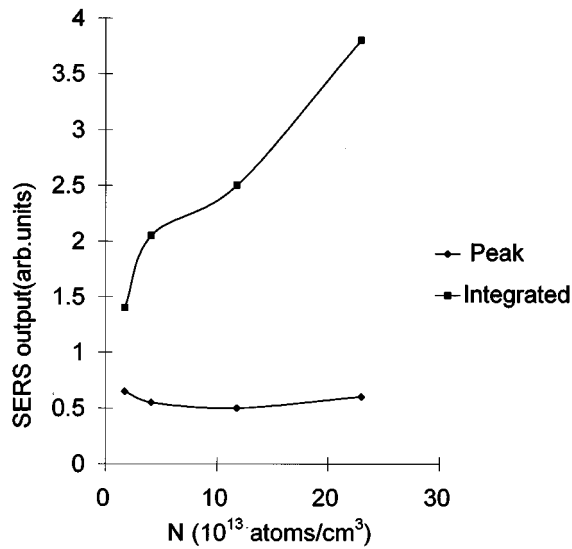
FIG. 10. SERS output versus number density. The lower curve shows the intensity measured at a peak corresponding to positive detuning. It shows saturation behavior. The upper curve is the integrated intensity corresponding to the entire tuning range. The cell length is 45 cm.

responsible for the output around 10^{13} atoms/cm^3. Beyond this density, once the Stokes field was strong enough, the system evolved to a CPT state. The fluorescence intensity at 451 nm monitored perpendicular to the tube axis versus the indium number density from the same cell is shown in Fig. 8. The density range A to B is the SR regime, C and beyond is the SERS regime where the fluorescence intensity drops. The drop in the fluorescence level and the SERS output beyond C are caused by the evolution of the system to a nonabsorbing CPT state.

The SERS output viewed on a screen appeared as a spot with graininess and speckle. It showed interesting variations in appearance with detuning as shown in Fig. 9. At the peak corresponding to positive detuning, the central spot is bright and well defined and at the peak corresponding to the negative detuning the central spot is more spread out and diffuse. These variations in the spot appearance are likely due to the changes in refractive index of the medium and the pump-induced focusing and defocusing of the Stokes light.

SERS output at the peak corresponding to the positive detuning versus the number density of indium using a 45-cm-long cell is shown in Fig. 10. It shows saturation behavior. Both atom depletion and pump depletion are responsible for the saturation behavior. At 25 μJ, the number of pump photons are 5×10^{13} per pulse. At a density of 10^{13} atoms/cm^3 the number of atoms in the path of the exciting column are nearly the same as the number of photons per pulse. Also atom depletion is expected since the final level $5P_{3/2}$ is metastable, the recycling time to reach the initial state $5P_{1/2}$ is large compared to the time duration of the pump pulse. However, the integrated intensity in the entire tuning range shown also in Fig. 10 is found to increase with the number density.

The maximum Raman conversion efficiency was found to be 40%. The range of tunability increased with increasing density of indium atoms and the length of the vapor column and found to be about 30 cm^{-1}. The tunability range [7]
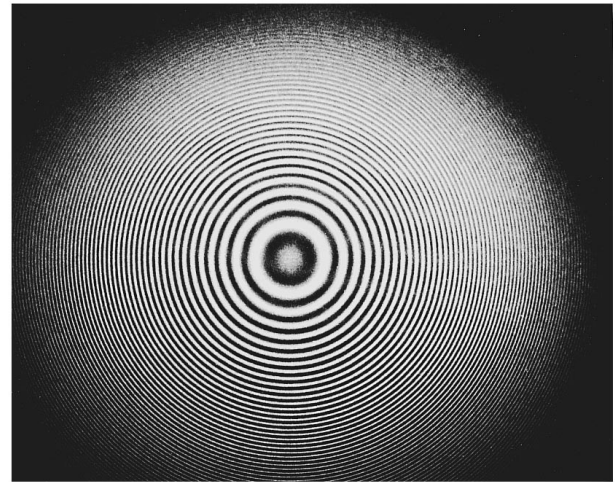
calculated using Eq. (1) agrees well with the observed experimental value. A Fabry-Pérot interferometer having a free spectral range of 2.5 cm^{-1} was used to measure the linewidth of the SERS output. The fringes are shown in Fig. 11. The measured linewidth is 0.9 cm^{-1}. This is significantly broader than the dye laser input or the Doppler broadened linewidth at 451 nm. Measurements of the SERS in alkali-metal vapors also showed a similar broadening of the Stokes output.

The polarization characteristics of the Stokes output were observed. The output was found to be equally strong both parallel and perpendicular to the polarization of the pump pulse. The Stokes radiation is generated within the medium; consequently, because of the high exponential gain, the Stokes output will have the polarization that experiences the maximum gain. The Stokes wave can take a general elliptical polarization, as was found also in cesium [7].

Tubes containing mixtures of indium and other inert gas-like atoms, mercury, cadmium, or zinc, were also used in this
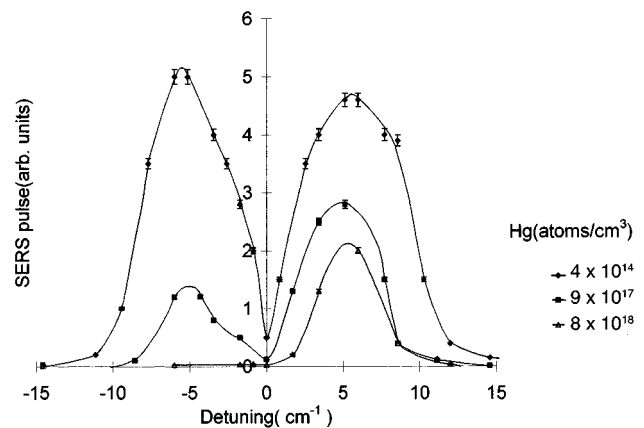

FIG. 11. Fabry-Pérot fringes of the SERS output. The interferometer has a free spectral range of 2.5 cm^{-1}.

FIG. 12. SERS pulse versus detuning. The indium mercury cell's length is 57 cm. The indium density is kept constant around 10^{13} atoms/cm^3. The three curves are for different mercury densities. Increasing the density of mercury has the effect of quenching the SERS output. There is an asymmetry in quenching, the peak corresponding to the negative detuning is quenched more rapidly.

study and were observed to produce stimulated electronic Raman scattering of indium. Figure 12 shows the SERS output from a 57-cm-long tube containing indium and mercury. The plots show the effect of mercury density on the output while the indium density is maintained constant around 10^{13} atoms/cm^3. Increasing the mercury densities has the effect of quenching the SERS output. The excimer (InHg) formation rate is expected to increase with increasing density of mercury, depleting indium atoms, and act as a source of competition with the SERS process. There is asymmetry in the quenching; the effect is more pronounced on the peak corresponding to the negative detuning from the line center, which gets almost completely quenched beyond a mercury density of around 10^{18} atoms/cm^3. This asymmetry is likely due to collisions with the mercury atoms and excimer formation. We know that the excimer potential corresponding to the atomic limit 6^2S lies below the limit and could have a pronounced influence on the SERS corresponding to the negative detuning. Other mixtures InCd and InZn showed similar features.

In summary, Dicke superradiance and stimulated electronic Raman scattering have been observed in indium vapor and our experimental results confirm the evolution of a coherent population trapping state. The simultaneous observation and measurement of the transverse fluorescence from the sample helped support our conclusions. The effect of inert gaslike atoms, mercury, cadmium, or zinc, on the SERS of indium was investigated. It would be interesting as a future project to carry out the theoretical modeling of processes occurring in different indium density regimes.

[1] R. H. Dicke, Phys. Rev. **93**, 99 (1954).

[2] N. Skribanowitz, I. P. Herman, J. C. MacGillivray, and M. S. Feld, Phys. Rev. Lett. **30**, 309 (1973); A. Flusberg, T. Mossberg, and S. R. Hartman, Phys. Lett. **58A**, 373 (1976); A. T. Rosenberger, S. J. Petuchowski, and T. E. DeTemple, in *Cooperative Effects in Matter and Radiation*, edited by C. M. Bowden, D. W. Howgate, and H. R. Robi (Plenum, New York, 1977), p. 15; M. Gross, C. Fabre, P. Pillet, and S. Haroche, Phys. Rev. Lett. **36**, 1035 (1976); M. S. Feld and J. C. MacGillivray, *Coherent Nonlinear Optics—Recent Advances*, edited by M. S. Feld and V. S. Letokhof (Springer-Verlag, Berlin, 1980), p. 73.

[3] M. Rokni and S. Yatsiv, Phys. Lett. **24A**, 177 (1967); M. Rokni and S. Yatsiv, IEEE J. Quantum Electron. **3**, 329 (1967).

[4] R. A. Wingarten, L. Levein, A. Flusburg, and S. R. Hartmann, Phys. Lett. **39A**, 38 (1972); D. Cotter, D. C. Hanna, P. A. Karkkainen, and R. Wyatt, Opt. Commun. **15**, 143 (1975); R. D. Varma, S. M. Jaywant, and Z. Iqbal, J. Opt. Soc. Am. B **2**, 403 (1985); M. G. Raymer and J. L. Carlsten, Phys. Rev. Lett. **39**, 1326 (1977).

[5] Y. Takubo, M. Tsuchiya, and M. Shimazu, Appl. Phys. **24**, 139 (1981).

[6] J. Migdalek, Can. J. Phys. **54**, 118 (1975).

[7] D. C. Hanna, M. A. Yuratich, and D. Cotter, *Nonlinear Optics of Free Atoms and Molecules*, Springer Series in Optical Sciences Vol. 17 (Springer-Verlag, Berlin, 1979), p. 187.

[8] G. Alzetta, A. Gozzini, L. Moi, and G. Orriols, Nuovo Cimento B **36**, 5 (1976); G. Orriols, *ibid.* **53**, 1 (1979); F. T. Hioe and C. Carroll, Phys. Rev. A **37**, 3000 (1988); S. Swain, J. Phys. B **15**, 3405 (1982); P. M. Radmore and P. L. Knight, *ibid.* **15**, 561 (1982); B. J. Dalton and P. L. Knight, *ibid.* **15**, 3997 (1982); G. S. Agarwal, Phys. Rev. Lett. **71**, 1351 (1993).

[9] I. V. Jyotsna and G. S. Agarwal, Phys. Rev. A **52**, 3147 (1995).